The constant-volume heat capacity of near-critical fluids with long-range interactions: A discussion of different Monte Carlo estimates

The constant-volume heat capacity of near-critical fluids with long-range interactions: A discussion of different Monte Carlo estimates

Christopher D. Daub, Philip J. Camp, and G. N. Patey

Citation: J. Chem. Phys. **118**, 4164 (2003); doi: 10.1063/1.1540630
View online: http://dx.doi.org/10.1063/1.1540630
View Table of Contents: http://jcp.aip.org/resource/1/JCPSA6/v118/i9
Published by the AIP Publishing LLC.

The constant-volume heat capacity of near-critical fluids with long-range interactions: A discussion of different Monte Carlo estimates

Christopher D. Daub
Department of Chemistry, University of British Columbia, Vancouver, British Columbia V6T 1Z1, Canada

Philip J. Camp
School of Chemistry, University of Edinburgh, West Mains Road, Edinburgh EH9 3JJ, United Kingdom

G. N. Patey[a)]
Department of Chemistry, University of British Columbia, Vancouver, British Columbia V6T 1Z1, Canada

(Received 8 August 2002; accepted 4 December 2002)

The constant-volume heat capacities, C_V, of various near-critical fluids with long-range potentials have been obtained using both canonical and grand-canonical Monte Carlo (GCMC) calculations. In the case of the restricted primitive model it is shown that the large discrepancies between previously reported results arise from the use of different simulation ensembles. In order to investigate how well the different ensemble estimates of C_V obtained with small systems can indicate the universality class of the bulk fluid, calculations have been performed for fluids with attractive pair interactions which vary like $-1/r^a$, with $a=6$, 4, and 3.1. For $a=6$, Ising-type criticality is expected, while for $a=4$ and 3.1 the criticality is mean-field. For each of these models the canonical-ensemble estimates of C_V do not provide unambiguous confirmation of the expected critical behavior, and hence this is not a reliable method for determining the universality class. This is also true of the GCMC estimates of C_V, which appear consistent with Ising-type behavior for all of the systems studied, even for those which are known to exhibit mean-field criticality in the thermodynamic limit. We suggest that these are artifacts associated with finite system size, and we speculate as to why they appear in canonical and GCMC calculations. © *2003 American Institute of Physics.* [DOI: 10.1063/1.1540630]

I. INTRODUCTION

The vapor–liquid critical behavior of ionic fluids continues to command considerable attention from experimental and theoretical groups alike.[1–3] The most significant issue has been whether the criticality of fluids with purely ionic interactions is Ising-type, mean-field, or neither. For the most part, the experimental study of the vapor–liquid transition in ionic fluids is complicated by the presence of other types of interactions. From a theoretical perspective, the most commonly studied model of ionic fluids in this context is the restricted primitive model (RPM), which consists of equal numbers of equi-sized positively and negatively charged hard spheres, interacting via the pair potential,

$$u(r)=\begin{cases}\infty, & r<\sigma\\ q_i q_j/Dr, & r\geqslant\sigma,\end{cases} \tag{1}$$

where r is the pair separation, σ is the hard-sphere diameter, q is the charge on ion i, and $D=4\pi\epsilon_0$, with ϵ_0 being the vacuum dielectric permittivity. Thermodynamic properties of the RPM are usually reported in reduced units, the most pertinent to the current discussion being defined as follows: the reduced temperature, $T^*=k_BTD\sigma/q^2$, with k_B being Boltzmann's constant; the reduced configurational energy, $U^*=U\,D\sigma/q^2$; the reduced number density, $\rho^*=N\sigma^3/V$, where N is the total number of ions, and V is the volume.

The location of the vapor–liquid critical point in the RPM is well established through many extensive simulation studies. In very recent work by Caillol *et al.*,[4] grand-canonical Monte Carlo (GCMC) simulations, histogram reweighting, and mixed-field finite-size scaling techniques were employed to study system sizes up to $L/\sigma=34$ (L is the cubic cell dimension). By assuming Ising-type criticality, and matching the probability distribution of the variable $x=(N-sU)/V$ to the universal distribution of the three-dimensional Ising model,[5,6] the position of the critical point was found to be $T_c^*=0.04917\pm0.00002$ and $\rho_c^*=0.080\pm0.005$, in excellent agreement with earlier estimates using somewhat smaller systems.[7–10] Further finite-size scaling analysis—without assuming Ising criticality—yielded estimates of the universal moment ratio $Q^*=0.63\pm0.01$, and correlation-length exponent $\nu=0.66\pm0.03$. These values compare favorably with those for the three-dimensional Ising model ($Q^*=0.623$[11], $\nu=0.630$[12]). The constant-volume heat capacity, C_V, along the locus χ_{NNN} (Ref. 13) was also presented in Ref. 4, but the results are not all what one would expect for a system with Ising-type criticality. Recall that upon the approach to an Ising-type critical point in three dimensions, the constant-volume heat capacity should diverge like $|T-T_c|^{-\alpha}$, with $\alpha=0.11$. In a finite-size simulation this divergence is rounded off, but one would at least expect a peak in C_V which increases and becomes more narrow with increasing system size. In contrast, Caillol *et al.*

a)Electronic mail: patey@theory.chem.ubc.ca

observe merely a shift and slight narrowing of the peak in C_V (see Fig. 11 in Ref. 4).

In recent work, Luijten, Fisher, and Panagiotopoulos[14,15] (LFP) have used GCMC simulations to investigate the critical behavior of a lattice version[16,17] of the RPM. Here we refer to the lattice-RPM model as the LRPM, and to the usual continuous case as simply the RPM. In Ref. 14, LFP present a detailed study of LRPM criticality using GCMC simulations, and unbiased finite-size extrapolation techniques.[13] The LRPM with a discretization parameter $\zeta = 5$,[16] exhibits a vapor–liquid critical point at $T_c^* = 0.050\,69 \pm 0.000\,02$, and $\rho_c^* = 0.0790 \pm 0.0025$ (the reduced units of the LRPM are the same as for the RPM). The measured effective susceptibility and correlation exponents, and an analysis of moment ratios, indicate Ising-type criticality, but rule out classical, *XY*, self-avoiding walk, and intermediate-range universality classes.

In Ref. 15, LFP calculate C_V in GCMC simulations of the LRPM with $\zeta = 5$, and the appropriate grand-canonical fluctuation formula,[18,13] containing terms arising from energy fluctuations and particle-number fluctuations, plus a cross term. The results are interesting in that they also indicate Ising-type critical behavior. Specifically, along a near-critical isochore ($\rho^* = 0.068$), C_V exhibits N-dependent maxima just below T_c (see Fig. 2 of Ref. 15). Peaks were found in C_V/Nk_B for systems as small as $L/\sigma = 6$ ($\langle N \rangle \simeq 15$), and are quite strongly pronounced at $L/\sigma = 10$ ($\langle N \rangle = 68$). These observations are surprising because they differ significantly with earlier canonical (NVT) Monte Carlo (MC) calculations of Valleau and Torrie[19,20] (VT) for the RPM, and the results recently reported by Caillol *et al.*[4] VT calculated C_V by fitting Padé approximants to the energy, and differentiating with respect to T, but no peak was apparent along a near-critical isochore (see Fig. 1 in Ref. 19).

To investigate these puzzling results, we have carried out a detailed analysis of the constant-volume heat capacity of the RPM and LRPM employing NVT-MC and GCMC calculations. In our NVT-MC simulations we calculate C_V using the standard energy-fluctuation formula, and by differentiating fits to the energy. C_V was calculated in our GCMC simulations using the appropriate fluctuation formula.[18,13] We repeat LFP's calculation of C_V in the LRPM using GCMC simulations; we find excellent agreement with the results of Ref. 15. Our NVT-MC results for the RPM extend those of VT both to significantly larger systems, and a wider range of temperatures; for systems of comparable size, our results are in excellent agreement with those of VT. Using our NVT-MC and GCMC results for the RPM, we show that the discrepancy between the C_V calculations of LFP and VT clearly come from the use of different ensembles.

To check that these results do not arise from some peculiarity of the RPM, we have also carried out the corresponding NVT-MC and GCMC calculations of C_V for fluids of hard spheres interacting *via* attractive pair potentials of the form,

$$u(r) = \begin{cases} \infty, & r < \sigma \\ -\epsilon(\sigma/r)^a, & r \geqslant \sigma, \end{cases} \tag{2}$$

where r is the pair separation, σ is the hard-sphere diameter as before, and ϵ is the well depth. In this model the reduced temperature is defined by $T^* = k_B T/\epsilon$; the reduced number density is as for the RPM. We have studied systems with $a = 6$, 4, and 3.1. These are interesting models because (at least in the infinite system limit) Ising-type criticality is expected for the $a = 6$ case, whereas fluids with $a = 4$ and $a = 3.1$ are expected to exhibit mean field behavior.[21–27] We draw particular attention to the extensive GCMC calculations and finite-size scaling analysis of Luijten and Blöte,[25] that confirmed classical critical behavior in three-dimensional ferromagnetic Ising models in which the interactions decay algebraically with exponents (in our notation) $a < 4.5$. Thus by comparing NVT-MC and GCMC results for these models, we get some indication as to how well the different estimates of C_V reflect the underlying universality class of the infinite systems. In earlier work[26] similar in spirit to the present effort, we used the same model fluids to identify signatures of non-Ising criticality as they appear in GCMC mixed-field finite-size scaling studies of relatively small systems.

This paper is organized as follows: In Sec. II we summarize the simulation methods used in this work. We present the results of NVT-MC and GCMC simulations of the RPM and the attractive hard sphere system in Sec. III, and the summary and conclusions in Sec. IV.

II. CALCULATIONS

NVT-MC and GCMC simulations were performed using cubic simulation cells of length L, in the normal way.[28] Ewald sums[28] were used to take account of the Coulombic interactions in the (L)RPM. All of the (L)RPM results we present were obtained with conducting boundary conditions ($\epsilon_s = \infty$), but calculations with vacuum boundary conditions ($\epsilon_s = 1$) were also carried out for three temperatures in the region of the critical point; no significant differences were found.

The simulations of the attractive hard-sphere systems were performed as described in Ref. 26. The pair potentials were spherically truncated at $L/2$, and the long-range contribution to the energy was calculated in the usual way, assuming the pair distribution function to be unity at particle separations greater than the cutoff radius.

In the following we use the notation $X(A,B)$ to represent the following quantity:

$$X(A,B) = \langle (A - \langle A \rangle)(B - \langle B \rangle) \rangle, \tag{3}$$

where $\langle A \rangle$ is the average value of the fluctuating variable A. In the NVT-MC calculations, C_V/Nk_B was obtained using both the fluctuation formula,

$$C_V = X(U,U)/k_B T^2, \tag{4}$$

and by fitting the average energies to a third-order polynomial in $\sqrt{T^*}$, then taking the temperature derivative. Tests were performed to ensure that the heat capacities obtained by the latter method were not overly sensitive to the nature of the fitting function; more complicated Padé approximant forms gave similar curves over the temperature ranges considered in this work. There is no doubt that NVT estimates of C_V for systems with long-range potentials will be prone to considerable finite-size effects. As an extreme illustration,

consider the energy fluctuations of a square-well fluid, in which the range of attraction is longer than $\sqrt{3}L/2$. Clearly, with a fixed number of particles the energy cannot change because each particle is within range of every other particle in the simulation cell, and the heat capacity will be zero. Of course, the Coulombic interaction does decay somewhat within the simulation cell, and in addition the energy can fluctuate by virtue of fluctuations in the charge ordering around the ions. Nonetheless, one must expect C_V calculated by the NVT route to be susceptible to finite-size effects, particularly near criticality. It would be a mistake, however, to assume that C_V calculated in GCMC simulations is immune to such effects, as we argue in the following.

In the GCMC calculations, C_V was calculated using the appropriate fluctuation formula,[18,13]

$$C_V = X(U,U)/k_B T^2 - X(N,U)^2/[X(N,N)k_B T^2]. \qquad (5)$$

The argument in favor of using GCMC calculations appears to be that fluctuations missing in small NVT systems due to the absence of a liquid–vapor interface might be better represented in GCMC calculations for systems of comparable size. However, the GCMC method would appear to have at least one potential pitfall. Both terms in Eq. (5) contain contributions that are related to the isothermal compressibility, κ_T. In an infinite system, as $T \to T_c$, κ_T diverges like $|T - T_c|^{-\gamma}$, with $\gamma = 1$ for mean-field criticality, and $\gamma = 1.24$ for Ising-type criticality. Thus, the terms in Eq. (5) diverge as $T \to T_c$ for both mean field and Ising universality classes; moreover, their divergences are much stronger than that expected for C_V in Ising-type systems. Of course for finite systems the terms in Eq. (5) are not truly divergent, but in the critical region they do become very large as N is increased. Clearly, the strongly ''divergent'' contributions to these terms must compensate exactly if the true behavior of C_V is to be obtained from Eq. (5) in a finite-size simulation. Unfortunately, the extent of finite-size effects on each of the functions $X(U,U)$, $X(U,N)$, and $X(N,N)$ in near critical systems is not known. One possibility is that in the rather small systems considered in MC calculations these fluctuations are suppressed to differing degrees such that the strongly divergent contributions to the terms of Eq. (5) do not compensate exactly. If this is the case, the estimated C_V curve might show a peak resulting from the strongly divergent (compressibility) contributions to Eq. (5), rather than from the weak divergence of energy fluctuations expected for Ising-type systems.

III. RESULTS AND DISCUSSION

Our results for both the LRPM (with $\zeta = 5$) and the RPM obtained at near-critical densities with $L/\sigma = 10$ are plotted as functions of $t = (T - T_c)/T_c$ in Fig. 1. The LRPM simulations were carried out at $\rho^* = 0.068$, the first estimated critical density reported in Ref. 15. We also performed calculations of the LRPM over the same temperature range at $\rho^* = 0.072$, the ''refined'' estimate added in proof in Ref. 15; only small differences in the heat capacities were observed. The RPM calculations were carried out at a reduced density of $\rho^* = 0.079$, which is within the range of recent estimates of ρ_c^*. The reduced critical temperatures and densities for the different models considered are summarized in Table I.

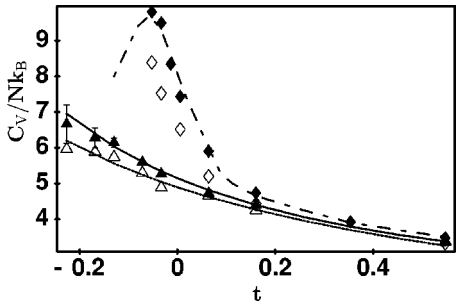

FIG. 1. The total heat capacity per ion as a function of temperature. All results shown are for $L/\sigma = 10$ with $\rho^* = 0.068$ (LRPM) and $\rho^* = 0.079$ (RPM). The error bars shown on several points represent one estimated standard deviation. The closed symbols and solid curve are for the LRPM with discretization parameter (Refs. 15 and 16), $\zeta = 5$. The closed triangles are NVT results obtained using Eq. (4). The solid curve was obtained by fitting the NVT energies and differentiating with respect to temperature. The open triangles and the dotted curve are RPM results obtained in NVT calculations. The open triangles were obtained using Eq. (4) and the dotted curve via an energy fit. The closed and open diamonds are our GCMC results for the LRPM and the RPM, respectively, obtained using Eq. (5). The dash-dot curve represents LFP's LPRM results from Fig. 2 of Ref. 15; we have added the kinetic contribution, 3/2, to their configurational values.

The comparisons made in Fig. 1 lead to two immediate conclusions. First, it is clear from the NVT-MC and GCMC results that the LRPM and the RPM are closely equivalent models, giving very similar heat capacities in a given simulation ensemble. Second, it is obvious that the NVT-MC and GCMC calculations give very different heat capacity curves in the vicinity of the critical point for both the LRPM and the RPM. The GCMC curves exhibit peaks near the critical temperature, as noted by LFP, whereas the NVT-MC curves are smoothly decreasing functions of t with no trace of a peak in the critical region, in agreement with the findings of VT. This ensemble dependence is clearly the origin of the discrepancy between constant-volume heat capacities reported by LFP and by VT. The GCMC results appear to suggest Ising-type behavior, whereas no evidence of this is apparent in the NVT-MC calculations. In view of this inconsistent behavior, one must ask how well these observations reflect the underlying criticality of the infinite systems of interest.

As discussed earlier, in an attempt to gain insight into this crucial question, we carried out NVT-MC and GCMC calculations of the heat capacity for three model systems with the interactions specified in Eq. (2), two of which are

TABLE I. Reduced critical temperatures and densities for the RPM, LRPM, and the models defined by Eq. (2). The numbers in parentheses denote the statistical uncertainty in the last digits.

Model	T_c^*	ρ_c^*	Reference
RPM	0.049 17(2)	0.080(5)	4
LRPM	0.051	0.068	15
LRPM	0.051 7	0.072	15 (note added in proof)
LRPM	0.050 69(2)	0.0790(25)	14
$a = 6$	0.597 2(1)	0.3757(4)	26
$a = 4$	1.372 4(1)	0.2993(1)	26
$a = 3.1$	11.452(8)	0.247(5)	26

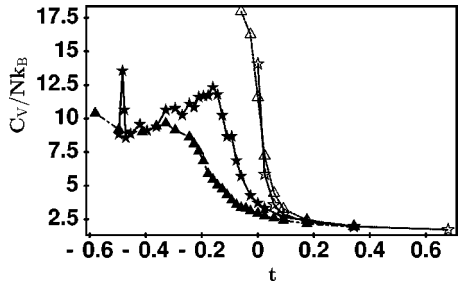

FIG. 2. The total heat capacity per particle for a fluid characterized by the pair potential defined by Eq. (2) with $a=6$. Results are shown as functions of temperature at the critical density (Table I). The closed triangles and stars are *NVT* results for $L/\sigma=6$ and $L/\sigma=10$, respectively, obtained using Eq. (4). The open triangles and stars are the GCMC results for $L/\sigma=6$ and $L/\sigma=10$, respectively, obtained using Eq. (5). The curves are drawn to guide the eye.

known to have mean field criticality ($a=4$ and $a=3.1$) and the other ($a=6$) Ising-type behavior. The critical temperatures and densities for these models are included in Table I. The heat capacities obtained for $a=6$, $a=4$, and $a=3.1$ are plotted as functions of t in Figs. 2, 3, and 4, respectively. For $a=6$ and $a=4$, we show the results of simulations with $L/\sigma=6$ and $L/\sigma=10$; for $a=3.1$ the results were extremely insensitive to system size, and so we only show results of simulations with $L/\sigma=10$.

For the $a=6$ system (Fig. 2) we see that both the *NVT*-MC and GCMC curves have peaks in the vicinity of $t=0$. Furthermore, the GCMC peaks move closer to $t=0$, and increase in height as L is increased; this is consistent with the expected Ising-type universality class. The *NVT*-MC results also exhibit peaks that move closer to $t=0$ and increase in height as L is increased. This behavior is also qualitatively consistent with Ising-type universality. However, one must be cautious in this interpretation because the triple point temperature for this system is $T_t^*\simeq 0.5$,[29] corresponding to $t\simeq -0.16$; this temperature is very close to the position of the peak in the $L/\sigma=10$ results. Therefore, it is probable that the peaks in the *NVT*-MC results have nothing to do with criticality, rather, they are likely related to the freezing transition for this system. The rather sharp peak at $t\approx -0.5$ occurring in the canonical curve for $L/\sigma=10$ is definitely related to ''freezing,'' inspection of configurational ''snapshots'' shows that the particles are associated into crystal-like clusters at this temperature.

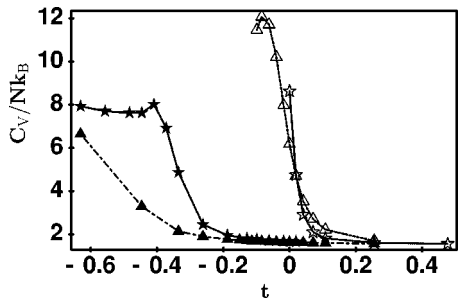

FIG. 3. The total heat capacity per particle for a fluid characterized by the pair potential defined by Eq. (2) with $a=4$. Results are shown as functions of temperature at the critical density (Table I). The symbols are as in Fig. 2.

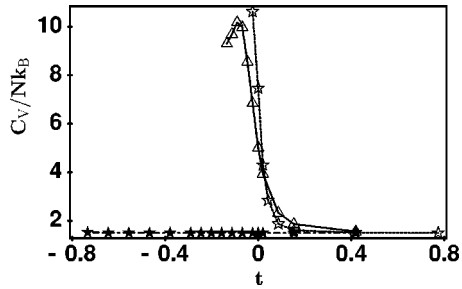

FIG. 4. The total heat capacity per particle for a fluid characterized by the pair potential defined by Eq. (2) with $a=3.1$. Results are shown as functions of temperature at the critical density (Table I). The symbols are as in Fig. 2.

The results for $a=4$ (Fig. 3) and $a=3.1$ (Fig. 4) are instructive. We see immediately that for both models, GCMC calculations continue to give strong peaks near $t=0$, and that the behavior of the curves with increasing L is very similar to that observed for $a=6$ and for the (L)RPM (see Fig. 1 and Ref. 15). Indeed, from the constant-volume heat capacities estimated using GCMC calculations one would be tempted to conclude that these systems are exhibiting signatures of Ising-type behavior, even though we know that at least in the infinite system limit these models fall into the mean field universality class. This suggests that caution is needed in interpreting the GCMC estimates of C_V obtained for small systems. The *NVT*-MC calculations, on the other hand, do not show any criticality related peaks in C_V for these models. For $a=4$ there is an apparent ''cusp'' at $t\simeq -0.4$ in the $L/\sigma=10$ case; however, this feature is far from $t=0$ and is likely related to freezing ($T_t^*=0.830$,[29] corresponding to $t=-0.40$); inspection of configurational ''snapshots'' indicates that the particles are associating into large clusters at this temperature. For $a=3.1$, the *NVT* curve remains rather flat and featureless throughout the critical region. We note that $T_t^*\simeq 5.6$,[29] corresponding to $t\simeq -0.5$, although no ''freezing'' peak is apparent in the simulation results for this system.

As was anticipated in Sec. II, C_V calculated in *NVT*-MC simulations is greatly suppressed but, as our results for the ''mean-field'' systems indicate, finite-size effects are also very significant in C_V calculated in GCMC simulations, in that Ising-type peaks are apparent even for systems that have mean-field criticality in the thermodynamic limit. Clearly, finite-size effects seriously compromise the reliability of C_V measurements as indicators of the universality class.

IV. SUMMARY AND CONCLUSIONS

In this paper we have demonstrated for several models that near the critical point, *NVT*-MC and GCMC estimates of the constant-volume heat capacity differ substantially. Since our calculations for the RPM and LRPM indicate that these systems have identical behavior within a given ensemble, this clearly must be a finite-size effect, and it explains why the C_V results reported by LFP for the LRPM differ so significantly from those obtained by VT for the RPM.

In an effort to assess the usefulness of the different estimates of C_V as indicators of the underlying universality class

of the system, we have carried out both *NVT*-MC and GCMC calculations for fluids of hard spheres with algebraically decaying tails. For the r^{-6} case, which is expected to be Ising-type, the heat capacities obtained in the canonical ensemble show peaked behavior in the vicinity of the critical point, but this is likely related to freezing rather than to criticality. For r^{-4}, the canonical-ensemble results show peaks far removed from the critical temperature that are likely due to freezing. No heat-capacity peak was observed in canonical-ensemble simulations of systems with $r^{-3.1}$ potentials.

On the other hand, along the critical isochore the GCMC curves show sharp peaks near T_c for all three models, including the two (r^{-4} and $r^{-3.1}$) which fall into the mean field universality class. Thus the presence of peaks in GCMC estimates of C_V does not appear to be a reliable signal of Ising-type criticality. Rather, we suspect that these peaks are an artifact associated with finite size, and are related to incomplete compensation of the strongly divergent contributions to the grand-canonical fluctuation formula for C_V.

Of course, one must hasten to add that the lack of peaks in the canonical-ensemble estimates of C_V for the RPM does not prove that the RPM does not fall into the Ising universality class. It may simply be that the systems considered are too small to give a reliable indication of the true behavior of C_V. Unfortunately, our calculations do show that GCMC calculations of the heat capacity C_V, employing small systems, likewise cannot serve as a basis for firm conclusions concerning the critical behavior.

ACKNOWLEDGMENTS

The authors thank John Valleau, Glenn Torrie, and Michael Fisher for useful discussions and correspondence. The financial support of the National Science and Engineering Research Council of Canada is gratefully acknowledged.

[1] M. E. Fisher, J. Phys.: Condens. Matter **8**, 9103 (1996).
[2] G. Stell, J. Phys.: Condens. Matter **8**, 9329 (1996).
[3] H. Weingärtner and W. Schröer, Adv. Chem. Phys. **116**, 1 (2001).
[4] J. M. Caillol, D. Levesque, and J. J. Weis, J. Chem. Phys. **116**, 10794 (2002).
[5] R. Hilfer and N. B. Wilding, J. Phys. A **28**, L281 (1995).
[6] M. M. Tsypin and H. W. J. Blöte, Phys. Rev. E **62**, 73 (2000).
[7] J. M. Caillol, D. Levesque, and J. J. Weis, Phys. Rev. Lett. **77**, 4039 (1996).
[8] J. M. Caillol, D. Levesque, and J. J. Weis, J. Chem. Phys. **107**, 1565 (1997).
[9] G. Orkoulas and A. Z. Panagiotopoulos, J. Chem. Phys. **110**, 1581 (1999).
[10] Q. Yan and J. J. de Pablo, J. Chem. Phys. **111**, 9509 (1999).
[11] H. W. J. Blöte, E. Luijten, and J. R. Heringa, J. Phys. A **28**, 6289 (1995).
[12] R. Guida and J. Zinn-Justin, J. Phys. A **31**, 8103 (1998).
[13] G. Orkoulas, M. E. Fisher, and A. Z. Panagiotopoulos, Phys. Rev. E **63**, 051507 (2001).
[14] E. Luijten, M. E. Fisher, and A. Z. Panagiotopoulos, Phys. Rev. Lett. **88**, 185701 (2002).
[15] E. Luijten, M. E. Fisher, and A. Z. Panagiotopoulos, J. Chem. Phys. **114**, 5468 (2001).
[16] A. Z. Panagiotopoulos and S. K. Kumar, Phys. Rev. Lett. **83**, 2981 (1999).
[17] J. M. Romero-Enrique, G. Orkoulas, A. Z. Panagiotopoulos, and M. E. Fisher, Phys. Rev. Lett. **85**, 4558 (2000).
[18] T. L. Hill, *Statistical Mechanics* (Dover, New York, 1987).
[19] J. Valleau and G. Torrie, J. Chem. Phys. **108**, 5169 (1998).
[20] J. Valleau and G. Torrie, J. Chem. Phys. **117**, 3305 (2002).
[21] G. Stell, Phys. Rev. B **1**, 2265 (1970).
[22] M. E. Fisher, S. Ma, and B. G. Nickel, Phys. Rev. Lett. **29**, 917 (1972).
[23] G. Stell, Phys. Rev. B **8**, 1271 (1973).
[24] M. Aizenman and R. Fernández, Lett. Math. Phys. **16**, 39 (1988).
[25] E. Luijten and H. W. J. Blöte, Phys. Rev. B **56**, 8945 (1997).
[26] P. J. Camp and G. N. Patey, J. Chem. Phys. **114**, 399 (2001).
[27] E. Luijten and H. W. J. Blöte, Phys. Rev. Lett. **89**, 025703 (2002).
[28] M. P. Allen and D. J. Tildesley, *Computer Simulation of Liquids* (Clarendon, Oxford, 1987).
[29] P. J. Camp, Phys. Rev. E (to be published).